Environmental Science
Water Research & Technology

ROYAL SOCIETY OF CHEMISTRY

PAPER

View Article Online
View Journal

Cite this: DOI: 10.1039/d0ew00314j

The impact of biofilm thickness-restraint and carrier type on attached growth system performance, solids characteristics and settleability

Raheleh Arabgol,[a] Peter A. Vanrolleghem,[b] Maria Piculell[c] and Robert Delatolla *[a]

Received 4th April 2020,
Accepted 31st July 2020

DOI: 10.1039/d0ew00314j

rsc.li/es-water

The moving bed biofilm reactor (MBBR) technology is a proven standalone and add-on technology for carbon and nutrient removal from municipal wastewaters. The key challenge of the carbon removal MBBR technology is the production of poor settling biological solids and the need for intense solid separation methods. This study investigates the effect of carrier type and biofilm thickness-restraint on MBBR system performance, biofilm thickness, solids production, detachment rate, solids characteristics and settleability. Two new emerging "thickness-restraint" carriers, AnoxK™ Z-200 and Z-400 (allowing for 200 and 400 μm maximum biofilm thickness, respectively), are compared to the conventional AnoxK™ K5 carrier at BOD loading rates of 6 g-sBOD m^{-2} d^{-1}. The obtained results indicate that carrier type has a significant effect on MBBR carbonaceous removal, biofilm thickness, detachment and solids production. The K5 carrier MBBR system demonstrated statistically significant higher carbonaceous removal rates of 3.8 ± 0.3 g-sBOD m^{-2} d^{-1}, higher biofilm thickness (281.1 ± 8.7 μm), lower solids production (7.7 ± 3.2 mg-TSS L^{-1}) and greater stability with respect to the detachment rate compared to the two Z-carriers. Particle size distribution analysis demonstrates a higher percentage of small particles in Z-carrier system effluent and hence significantly lower solids settling efficiency. Therefore, the K5 carrier produced solids with improved settling characteristics compared to Z-carriers. No significant difference was observed in removal efficiency, solids production, detachment rate, particle characteristics and settling behaviour when comparing the Z-200 to the Z-400, indicating that biofilm thickness-restraint carrier design was not a controlling factor in the settling potential of produced solids.

Water impact

The poor settleability of biologically produced solids from the widely applied MBBR wastewater treatment technology remains a key challenge. This study characterizes MBBR effluent solids and demonstrates the effects of carrier type and limiting biofilm thickness *via* specifically designed carriers on system performance, effluent solids size distribution and solids settling. The study relates observed solids characteristics to measured settleability.

Introduction

New regulations and more stringent wastewater discharge standards are increasingly enforced due to a raised awareness regarding the detrimental effects of wastewater discharge into surface water bodies.[1,2] Therefore, wastewater treatment facilities are being required to improve their treatment and reduce the concentration of organic matter, nutrients and solids prior to discharge.[3] In order to improve the quality of treated wastewater, the use of advanced, cost-effective and efficient technologies is required to upgrade or replace ageing, existing wastewater treatment infrastructure.[1,4–8] In this regard, the carbon removal moving bed biofilm reactor (MBBR) technology is a proven, compact, standalone biological treatment unit and a means to upgrade passive and conventional wastewater treatment systems.[7–10] The MBBR system is an attached growth biological treatment process that was developed approximately 25 years ago by Kaldnes Miljøteknologi, as a robust reactor with no need for sludge recirculation and backwashing.[11,12] High load tolerance, elevated biomass maintained in a small footprint, high treatment efficiency, cost and energy effectiveness, low vulnerability to cold temperature, low operational intensity and

[a] *Department of Civil Engineering, University of Ottawa, 161 Louis Pasteur, K1N 6N5, Ottawa, Canada. E-mail: robert.delatolla@uottawa.ca*
[b] *ModelEAU, Département de génie civil et de génie des eaux, Université Laval, 1065 av. de la Médecine, Québec, Canada*
[c] *AnoxKaldnes - Veolia Water Technologies, Klosterängsvägen 11A, 226 47 Lund, Sweden*

low sludge production are additional advantageous characteristics of this technology.[2,4,8,13–18] With these advantageous characteristics, it should be noted that relatively poor settleability of biologically produced solids in carbon removal MBBR effluent is a potential drawback and remains a concern of the MBBR technology compared to conventional suspended growth systems.[10,12,19,20] Several studies have highlighted the necessity of using intense solids separation methods (such as filtration, lamella settling, or using enhanced sedimentation with pre-coagulation) due to the poor settling characteristics of the biomass leaving MBBR systems.[19,20]

The MBBR technology relies on freely moving plastic carriers with a high surface area that provides a substratum for bacterial growth and maintenance. The carriers are exposed to other carriers, interaction with aeration, and the surrounding liquid in the MBBR reactors. As the exposure to the shear forces in the reactor affects the biofilm thickness and quantity of attached biomass along with the potential characteristics of the dispersed and detached solids, the physical characteristics of the carriers in the MBBR technology likely play a considerable role on solids production, characteristics and the settleability of these particles.[11,21]

The effective carrier surface area is an important parameter in MBBR design. A higher effective surface area of a carrier will promote a higher biofilm surface area for the same quantity of carriers and hence will augment the performance of a system with a specified reactor volume or will allow for the design of a smaller reactor volume at the same reactor performance. Therefore, over the years, different types of carriers (of different material, shape, and size) have been developed and still are being modified to improve removal efficiency by providing a higher effective surface area.[12,22] Several studies performed individually on various carriers have evaluated organic matter removal, ammonia removal and solids production of MBBR reactors to treat various types of wastewaters.[23–27] Previous studies demonstrated that the physical and geometrical properties of the carriers play an important role in wastewater hydrodynamics and oxygen transfer efficiency in the MBBR reactors,[28] which ultimately might contribute to reactor performance. Where similar performance results have been observed in the investigation of various media for biofiltration.[29] The previous studies on MBBR systems have mainly focused on how the removal efficiency and solids production change as a result of different surface area loading rate (SALR), hydraulic retention time (HRT), temperature and filling degrees of the carriers.[8,23,30,31] Research has demonstrated that MBBR carbon removal efficiency depends on the effective surface area that is available for biomass growth regardless of carrier type and shape.[21,30,32–35] Particle characteristics and especially particle size distribution along with the settleability of the particles in MBBR effluent have shown a good correlation with HRT and SALR.[10,17,20,21,36] Enhanced settleability of MBBR effluent solids has been demonstrated at lower SALR and, consequently, longer HRT due to larger particle sizes.[10,20] Moreover, a significant difference has been demonstrated between the settleability and the characteristics of the solids for different types of carriers when high loading was applied, and the carrier was clogged.[8,33] Although previous studies have proven that the carrier material and substratum surface properties have a significant effect on biofilm formation rate, biofilm distribution pattern and biofilm thickness;[22,37–40] there remains uncertainty regarding the impact of physical and geometrical characteristics of carriers on MBBR system performance, solids production and settling potential of suspended solids associated to different carrier types. Moreover, it is not well understood how the biofilm thickness affects system performance and solids characteristics regardless of the carrier type.

Furthermore, carriers have been shown to suffer clogging due to uncontrolled biofilm growth, with the effective surface area of the system becoming considerably decreased and the performance of the system being negatively impacted. Moreover, the uncontrolled growth of biofilm may lead to heavier carriers and hence systems that require more energy for mixing and more consumption of oxygen by the inactive and thick biofilm.[41] Therefore, to avoid potential negative impacts of clogging on MBBR performance, researchers were encouraged to develop new types of carrier to control the biofilm thickness and decrease the difference between the exposed biofilm area (EBA) and the effective surface area used for design.[42]

Recently, a new series of carriers (AnoxK™ Z-carriers) have been designed to control and maintain the thickness of the biofilm to a predetermined maximum thickness.[12,22,40] Before the invention of the Z-carriers, evaluating the direct effect of biofilm thickness on the MBBR system performance was not possible. Currently, there is limited research on nitrogen removal, carbonaceous removal and calcium scaling effects using the "thickness-restraint" carriers.[40,42] Controlling biofilm thickness may impact the detachment mechanism of biological mass from the carriers and hence impact the effluent solids and, ultimately, their settleability. Although some studies have indicated that different operational conditions (such as SALR, HRT, C/N ratio and temperature) can change the thickness of biofilm and the quantity of biomass in the reactor and hence the overall MBBR system performance;[8,23,30,31] there are no studies to date that demonstrate how controlling the biofilm thickness affects the MBBR system performance along with the solids production, detachment rate, particle characteristics and settleability, conversely.

Based on the literature, it is hypothesized that an enhanced understanding of the impact of various carrier types and the use of newly designed thickness-restraint carriers can be used to optimize the design of MBBR systems and their subsequent downstream solids separation units. Therefore, this study aims to improve the current understanding of the effects of carrier type and newly designed thickness-restraint carriers on the kinetic performance of MBBR systems, the effluent solids characteristics and subsequent downstream solids settleability. In particular, the objective of this study is to investigate the

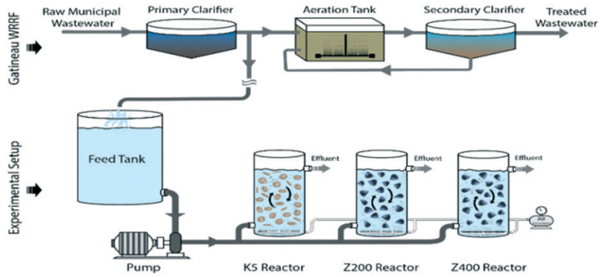

Fig. 1 Experimental set-up.

effects of different types of carriers, the conventional AnoxK™ K5 carrier compared to the newly designed "thickness-restraint" AnoxK™ Z-carriers, as well as the effect of biofilm thickness-restraint on carbonaceous removal rates (soluble biological oxygen demand (sBOD) and soluble chemical oxygen demand (sCOD)), total ammonia nitrogen (TAN) removal rates, effluent solids, effluent particle size distribution and characteristics, and effluent solids settleability.

Materials and methods

Experimental setup

This study was conducted at the Gatineau municipal secondary treatment water resource recovery facility (WRRF), Quebec, Canada. Three identical laboratory-scale MBBR reactors with volumes of 4 L were operated in parallel. A reservoir feed tank was used to collect the primary clarified wastewater and distribute it to the reactors to ensure constant flow rates of 3.7 ± 0.1 L h^{-1} in the reactors (Fig. 1).

The reactors housed three different types of carriers; the conventional AnoxK™ K5 carrier and two types (AnoxK™ Z-200 and AnoxK™ Z-400) of newly designed "thickness-restraint" Z-carriers (AnoxKaldnes, Lund, Sweden). It should be noted that in order to maintain similar carrier surface areas and loading rates in the three reactors, within conventional ranges, different number of carriers were housed in each of the reactors (Table 1). In addition, it is noted that the carrier fill percentage of all reactors in this study was maintained below maximum fill percent capacities.

Carrier characteristics

Two different types of carriers, conventional K5 carrier and newly designed Z-carriers, were used in this study. The conventional K5 carrier is a porous cylindrical carrier (Table 1), which is a commonly used carrier in full-scale carbonaceous and nitrogen removal applications.[30] The saddle-shaped Z-carriers, on the other hand, are a newly designed carrier to control biofilm thickness, and as such, they are significantly different in shape compared to the conventional K5 carrier (Table 1). Z-Carriers are covered with a grid of specific height, allowing the biofilm to grow on the outside of the carrier in a protected compartment rather than biofilm growing inside the protected inner voids of K5 carriers.[42] Therefore, Z-carriers limit the maximum thickness of the biofilm growth on the carrier to the height of the predefined carrier's grid wall. The excess biomass could scrape off due to abrasion caused by the collision between carriers in the reactor and also due to erosion caused by hydraulic shear forces acting on the biofilm attached to the carriers.[12,42] The Z-200 and Z-400 carriers are identical in shape and provide a similar exposed biofilm area (EBA) of 1280 mm^2 per carrier and a projected diameter of 30 mm (with the two types of Z-carriers having different grid wall heights). While the cylindrical K5 carrier has a diameter of 25 mm and a height of 3.5 mm and provides a surface area of 2420 mm^2 per carrier (Table 1).[12,42] In this study, the Z-200 and Z-400 carriers, with grid wall heights of 200 and 400 μm respectively, were used to study the effects of the thickness-restraint on system performance. In particular, the biofilm thickness on the Z-200 carriers is restrained to a predefined thickness of 200 μm compared to the Z-400 carriers that are allowed to increase in thickness up to 400 μm.

Wastewater characteristics

Primary clarified municipal wastewater from the city of Gatineau WRRF (Table 2) was used as influent for all of the MBBR reactors operated in this study. The primary clarifiers of the WRRF were conventional sedimentary basins and were operated without chemical addition. Although coagulant is not added during primary clarification, the raw municipal wastewater (Table 2) entering the Gatineau WRRF includes reject water from three water treatment plants servicing the

Table 1 Reactor properties at SALR of 6.0 ± 0.8 g-sBOD m^{-2} d^{-1}

	Reactor volume (L)	No. of carriers	Carrier surface area[a] (mm^2 per carrier)	Reactor surface area (m^2 per reactor)	Carrier image
K5	4	160	2420	0.38	
Z-200	4	300	1280	0.38	
Z-400	4	300	1280	0.38	

[a] Protected surface area (PSA) for K5, and exposed biofilm area (EBA) for Z-carriers.[42]

Table 2 Characteristics of raw wastewater entering the Gatineau WRRF and the clarified feed wastewater entering the on-site MBBR reactors

Constituent	Raw influent wastewater[a] Average ± 95% CI	Clarified wastewater entering MBBRs[b] Average ± 95% CI
TSS (mg L^{-1})	212.7 ± 12.2	49.3 ± 4.2
VSS (mg L^{-1})	207.5 ± 12.2	38.1 ± 2.4
COD (mg L^{-1})	233.6 ± 10.2	118.8 ± 6.8
BOD (mg L^{-1})	100.5 ± 5.1	53.6 ± 4.4
sCOD (mg L^{-1})	NA	58.7 ± 4.5
sBOD (mg L^{-1})	NA	23.0 ± 2.4
TAN (NH_3/NH_4^+–N mg L^{-1})	15.6 ± 0.5	16.0 ± 0.9
Nitrite (NO_2^-–N mg L^{-1})	0.0 ± 0.0	0.0 ± 0.0
Nitrate (NO_3^-–N mg L^{-1})	1.0 ± 0.2	2.7 ± 0.1
VSS/TSS ratio (%)	97.5 ± 0.7	79.3 ± 2.7
COD/BOD	2.5 ± 0.1	2.3 ± 0.1
sCOD/sBOD	NA	2.7 ± 0.2
Temperature (°C)	15.0 ± 1.0	15.0 ± 1.0
DO (mg L^{-1})	NA	2.1 ± 0.6
pH	7.3 ± 0.0	7.7 ± 0.1

[a] Average and 95% confidence interval (95% CI) across the study ($n \approx 365$). [b] Average and 95% confidence across the study ($n \approx 50$). NA: not available.

community. Therefore, the residual alum in the reject water is a portion of the WRRF raw wastewater and, as such, may affect solids removal in the primary clarifiers. The primary clarifiers demonstrated approximately 76% total suspended solids (TSS) removal throughout the experimental phase, prior to entering the MBBR reactors. The influent characteristics of this study are in the range of typical strength raw wastewater for Canadian WRRFs.

Biofilm inoculation and start-up

All carriers were inoculated with non-diluted, return activated sludge (RAS) harvested from the Gatineau WRRF. The TSS and volatile suspended solids (VSS) concentrations of the RAS and hence within the reactors during inoculation were 9.2 g-TSS L^{-1} and 6.8 g-VSS L^{-1}. The reactors were operated in batch mode, housing virgin carriers, for one week with RAS wastewater. Following one week of operation with RAS as batch reactors, when biofilm growth was observed on the carriers, the reactors were continuously fed with primary clarified wastewater (Table 2) for a continued inoculation period of four additional weeks with increasing flow rates up to 3.7 L h^{-1}. Subsequently, the reactors were operated at the experimental conditions with a flow rate of 3.7 L h^{-1} and a loading rate of approximately 6 g-sBOD m^{-2} d^{-1} for another three weeks (with three weeks equal to 504 times HRTs) to monitor the biofilm development, maturation and acclimatization on the carriers. The MBBR reactors were deemed to be fully inoculated once the systems demonstrated steady-state operation (after three weeks of operation at 3.7 L h^{-1} and 6 g-sBOD m^{-2} d^{-1}). The steady-state operation was validated within all the MBBR reactors by ensuring a maximum of ±15% variance of carbonaceous removal rates, changes in biofilm thickness and changes in biofilm mass per carrier across time.

Reactor operation

During the experimental phase of the study, 15 months, the three reactors were fed from the same feed tank with identical flowrates of 3.7 ± 0.1 L h^{-1} and an identical HRT of 1.1 h. Approximately 14 m^3 d^{-1} (≈10 litres per minute (LPM)) of aeration was supplied to each of the reactors by an air compressor and air diffusers located at the bottom of each reactor (Fig. 1). The number of carriers in the three reactors was modified during the experimental phase; specifically, carriers were removed from the three reactors to provide a range of operational SALR values and responses to best evaluate the carbonaceous removal kinetics of the carriers. The range of carbonaceous SALR was 0.7 to 9.3 g-sBOD m^{-2} d^{-1}, and the range of TAN SALR was 0.6 to 5.2 g-TAN m^{-2} d^{-1}. All three reactors were operated at a set carbonaceous SALR of 6.0 ± 0.8 g-sBOD m^{-2} d^{-1} and TAN SALR of 4.1 ± 0.3 g-TAN m^{-2} d^{-1} to compare carbonaceous removal kinetics and solids characteristics at the same loading rates. At this operational condition, which corresponds to a conventional loading rate for MBBR systems,[18,20] the reactors were tested for biofilm thickness, solids production, detachment rates, particle characteristics and settleability to compare the three reactors at the same operational condition.

At a carbonaceous SALR of 6.0 ± 0.8 g-sBOD m^{-2} d^{-1} and TAN SALR of 4.1 ± 0.3 g-TAN m^{-2} d^{-1}, the reactors housed surface areas for biofilm attachment of 0.38 m^2 per reactor; with 160 K5 carriers and 300 of Z-200 and Z-400 carriers being housed in the reactors (Table 1). All three reactors were operated in parallel with non-limiting dissolved oxygen (DO) conditions and sufficient aeration to ensure movement of the carriers in the reactors. The DO concentration ranged between 6 to 7 mg L^{-1} for the three reactors, which is above conventional values of 4 mg L^{-1} as slightly higher aeration rates were required to keep the carriers in motion within the laboratory-scale sized reactors used in this study. Moreover, pH and temperature were maintained at 7.8 ± 0.1 and 18.0 ± 1.0 °C, respectively, throughout the experimental period.

Constituent analytical methods

Influent and effluent grab samples were collected from the reactors and analyzed for the following parameters throughout the study: total BOD and sBOD, total COD and sCOD, TSS, VSS, TAN, nitrite, nitrate, DO, pH and temperature. The grab samples were taken two to three times a week during data collection periods and tested in triplicate within 4 hours of collection. The average of the triplicated measurements is reported in this study. The following methods were used to analyze total and soluble BOD, all nitrogen constituents and solids in accordance with standard methods: 5210B-5 day BOD, 4500-NH_3, 4500-NO_3^-, 4500-NO_2^-, 2540D-TSS (TSS dried at 103–105 °C) and 2540E-VSS (fixed and volatile solids ignited at 550 °C). A HACH DR 5000 Spectrophotometer (HACH, Loveland, CO, USA) was used to determine total and soluble COD concentrations according to HACH methods 8000. DO, pH and temperature were measured using an HQ40d portable PH/DO meter (HACH, USA).

Solids analysis

In addition to TSS and VSS concentration measurements, further calculations were performed to quantify the solids production and the solids detachment rate. As the HRT of the MBBR reactors is short (1.1 h) in this study, it can be assumed that the influent particles remain unchanged, and the effects of hydrolysis of the particles in the reactors is negligible. Therefore, the TSS production is calculated as the difference between the effluent TSS and the influent TSS. Moreover, the detachment rate is defined as the difference between the MBBR influent and effluent TSS, normalized per surface area of carriers in the reactor.

Biofilm thickness analysis

The biofilm thickness was measured by acquiring top view stereomicroscopy images of the void spaces of the K5 carriers and cross-sectional images of the cut compartments of the Z-carriers due to the different shape of the carriers. Images were obtained using a Zeiss Stemi 305 stereoscope (Toronto, Canada), and the acquired images were analyzed using the Fiji open-source software (http://fiji.sc/Fiji).[43] Three different randomly selected carriers were harvested from each reactor and imaged within 1 hour to minimize the potential effects of biofilm dehydration. The biofilm thickness was measured using fresh, wet biofilm but not biofilm submersed in liquid. The biofilm thickness reported in this study is the average height of the biofilm growth on the surface of the carriers. The average height of the biofilm was calculated by measuring the top view occupied area by biofilm over the length of the available surface for the biofilm. The occupied area of the biofilm is the integrated area between the substratum and the bulk-liquid interface (Fig. 2). The biofilm thickness for at least one side of all 64 void spaces of K5 carriers were imaged and analyzed. On the other hand, to achieve a better vision of biofilm thickness on Z-carriers, the longest strip was cut to acquire cross-sectional images and analyzed for both sides of all the cut compartments, including compartments close to the edges as well as the compartments in the center of the carriers. The average of all measurements ($n \approx 160$) was reported as the overall average of biofilm thickness per carrier with deviation based on a comparison between average thicknesses measured for the carriers.

Particle size distribution analysis of solids

Along with the chemical constituent testing, a micro flow imaging (MFI) technology was used to quantify the number of particles, particle size, concentration, area and circularity coefficients of the particles in the MBBR reactors. In particular, a Brightwell Technologies dynamic particle analyzer (DPA) equipped with a BP-4100-FC-400-Uflow cell (Brightwell Technologies, Canada, ON) was operated at low magnification to observe and quantify particles in the range of 2.25–400 μm in diameter according to Forrest *et al.* (2016)[33] and Karizmeh *et al.* (2014).[10] The acquired DPA images were analyzed to determine particle properties based on the two-dimensional projection of the particles by the analyzer. The volume of the particles was calculated using $\pi(\mathrm{ECD})^3 \times \mathrm{circularity}/6$. ECD is defined as the equivalent circular diameter and is based on the assumption that all the particles are spheres. ECD is equal to the diameter of a circle with an equivalent area of the irregular shaped particle, calculated as $2 \times (\mathrm{area}/\pi)^{0.5}$. Circularity is defined as the perimeter of the equivalent area circle divided by the perimeter of the actual particle. This dimensionless number varies between zero (for noncircular particles) and 1 (for circular particles).[10,33]

Finally, the DPA graphs are displayed in this study as the percent volume of particles across particle size. The integrated area under the particle distribution curves reveals the total volume percentage of unsettled particles in the sample. Therefore, the settleability is calculated as the percentage of total solids that are settled during a specific settling time. In this study, solids distribution samples were analyzed before and after 4 hours of settling to mimic the secondary clarifier retention time at the full-scale WRRF, where the reactors in this study were operated. Particle size distribution was analyzed to investigate the effects of carrier type and biofilm thickness-restraint on particle characteristics and settleability of particles. The particle distribution of effluent MBBR samples was measured in triplicate throughout the study during the steady-state operation of each system.

Statistical analysis

The student *t*-test was used to validate significant statistical differences between the measured constituents, the solids concentration, solids production and detachment rates, with a *p*-value less than 0.05 indicating significance in this study.

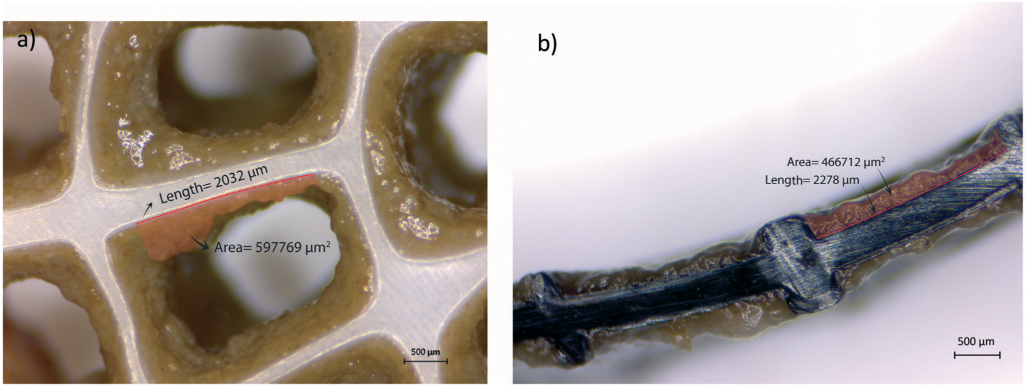

Fig. 2 a) Top view occupied area of biofilm in one void of the K5 carriers and b) cross sectional images of biofilm thickness in a compartment of Z-carries.

Average and 95% confidence intervals (95% CI) shown as error bars are displayed in all figures.

Results and discussion

Reactor carbonaceous and ammonia removal performance

Carbonaceous removal (sBOD and sCOD) along with TAN removal by the three MBBR reactors were quantified across numerous loading conditions and a maintained HRT at 1.1 hours to determine the effects of carrier type and thickness-restraint on system performance (Fig. 3). Due to the short HRT of the MBBR technology, and the lack of a settling unit in this study, the carbonaceous material is tracked in the soluble phase. The concentration of carbonaceous substrate in the influent wastewater was 58.7 ± 4.5 mg-sCOD L^{-1} and 23.0 ± 2.4 mg-sBOD L^{-1} with the sCOD to sBOD ratio of 2.7 ± 0.2. The carbonaceous surface area removal rate (SARR) across the SALR demonstrated a strong linear correlation between the measured sBOD loading rate and the removal rate (Fig. 3a) in all three reactors ($0.79 < R^2 < 0.94$). As such, all three reactors demonstrate first order sBOD kinetics and sBOD mass transfer rate limited conditions, likely due to the low loading rate of the substrate.[18] Similar conditions are also commonly observed in full-scale MBBR carbonaceous removal installations.[18,32,44,46] The substrate removal performance in attached growth wastewater systems, including the MBBR technology, is mediated by the mass transfer of the substrate (carbonaceous matter or nutrients) or the electron acceptor (DO) from the bulk liquid to the biofilm surface and subsequently through the biofilm itself to the embedded biomass. The linear relation in this study between the sBOD SARR and the sBOD SALR values are indicative that the sBOD SARR is limited by the mass transfer effects of the carbonaceous matter. The order of the sBOD kinetics of these attached growth MBBR systems has been shown to shift from sBOD mass transfer-dependent (first-order relation) to DO mass transfer-dependent (zero-order relation) at increased sBOD SALR values to the DO aeration rates.[18,30,45]

Moreover, a linear correlation and first-order kinetics were also observed for sCOD removal rate with respect to loading rate (Fig. 3b). Unlike the carbonaceous removal rate, a weak correlation is detected between the measured TAN loading rate and removal rate (Fig. 3c), likely due to the pathway of TAN removal being *via* assimilation by microorganisms. The lack of nitrification in the system, as is evident by the not remarkable change in influent and effluent NO_x concentrations, is likely due to the heterotrophic community outcompeting the nitrifying autotrophic community. BOD to total Kjeldahl nitrogen (TKN) ratios larger than 1.0, influent sBOD concentrations larger than 12 mg L^{-1} and organic loads above 5 g-sBOD m^{-2} d^{-1} are known to limit the TAN removal in MBBR reactors *via* heterotrophs outcompeting the nitrifying autotrophs.[46,47] The BOD to TAN ratio of this study was 1.4 ±

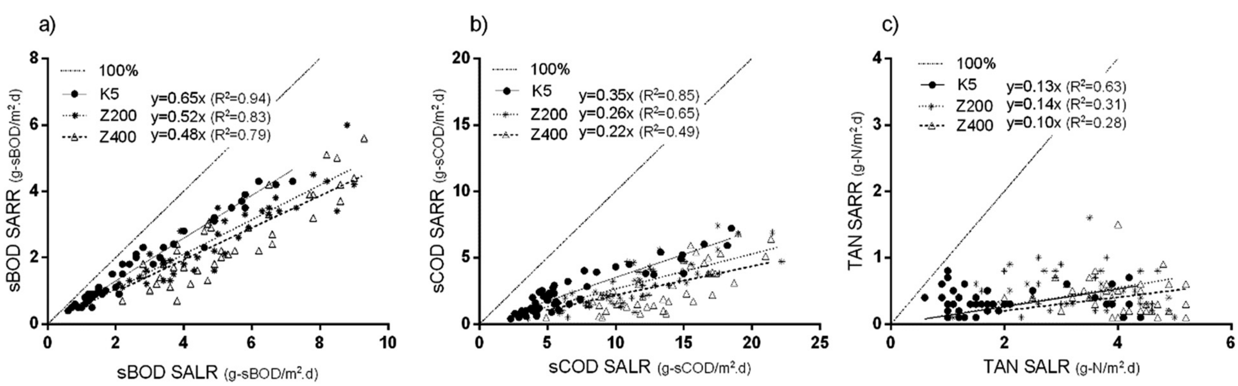

Fig. 3 SARR *versus* SALR across a range of loading rates for various carriers with respect to (a) sBOD (b) sCOD and (c) TAN removal.

0.1, assuming that organic nitrogen concentrations do not contribute to nitrification, the influent sBOD was 23.0 ± 2.4 mg-sBOD L^{-1}, and the organic load studied for biofilm and solids responses was 6 ± 0.8 g-sBOD m^{-2} d^{-1}; hence nitrification was limited in this study. The results demonstrate that the carrier type (*i.e.*, the physical properties of the carriers) has a statistically significant impact on the carbonaceous removal performance, as demonstrated by the sBOD and sCOD kinetics across different loading conditions (Fig. 3a and b). Although the DO concentrations in this study were elevated compared to conventional values, the elevated DO concentrations likely results in improved carbonaceous removal rates for the three carrier types due to the similar DO concentrations and mixing configuration of the three reactors. At a selected operational SALR of 6.0 ± 0.8 g-sBOD m^{-2} d^{-1}, the measured sBOD and sCOD SARR values and removal efficiencies also demonstrate that carbonaceous removal performance is significantly affected by carrier type (Fig. 4a and b). Cylindrically shaped K5 carriers with protected biofilm show significantly better removal rates and removal efficiencies in terms of sBOD and sCOD ($p < 0.05$) as compared to the saddle-shaped Z-carriers with exposed surface biofilm. Therefore, the K5 carrier with a SARR of 3.8 ± 0.3 g-sBOD m^{-2} d^{-1} (or 5.0 ± 0.7 g-sCOD m^{-2} d^{-1}) and 59.9 ± 3.0% sBOD removal efficiency (or 31.5 ± 4.0% sCOD removal efficiency) shows statistically significantly higher removal rates compared to the Z-carriers. 45 to 80% better sCOD SARR is observed for K5 as compared to Z-carriers, which implies a significant effect of carrier type on carbonaceous removal. However, TAN removal rates and efficiencies are not significantly different across carrier type ($p > 0.05$), likely due to the low TAN removal performance of the systems and the likely pathway of removal being cell assimilation. The changes in NO_x concentration were not remarkable between influent and effluent of the reactors and TAN : sCOD removal ratio varies between 7 and 14%, which is consistent with theoretical TAN : COD ratios of cell synthesis for aerobic hetrotophs.[48] This ratio of removal supports the hypothesis that nitrification was not occurring in the reactors, and the low TAN removal is likely due to nitrogen assimilation by heterotrophic microorganisms. The TAN removal rate was approximately 0.4 ± 0.1 g-TAN m^{-2} d^{-1} in all three reactors, and the removal efficiency was between 9.1 ± 2.6% and 11.1 ± 3.0% (Fig. 4c).

A comparison of the performance of the Z-200 carriers to the Z-400 carriers demonstrates that restraining the thickness of the Z-200 carriers compared to the Z-400 carriers did not affect the overall removal rates or efficiencies of the systems. An SARR of 2.9 ± 0.4 g-sBOD m^{-2} d^{-1} (or 3.4 ± 0.7 g-sCOD m^{-2} d^{-1}) and 2.6 ± 0.5 g-sBOD m^{-2} d^{-1} (or 2.8 ± 0.8 g-sCOD m^{-2} d^{-1}) was observed for Z-200 and Z-400, respectively. Therefore, the thickness-restraint did not show any significant effect for either carbonaceous or TAN removal rates and efficiencies.

Biofilm thickness

The thickness of the biofilm was characterized at the loading rate of 6.0 ± 0.8 g-sBOD m^{-2} d^{-1} to investigate the effects of carrier type and thickness-restraint on biofilm thickness and hence solids production, characteristics and settleability. The thickest biofilm was observed on K5 carriers (281.1 ± 8.7 μm), which can be explained by the protected and non-limited area for biofilm growth inside the voids of the carrier as opposed to the exposed surface area for biofilm growth of the Z-carriers. The overall average biofilm thickness on the Z-carriers was approximately 111.6 ± 11.3 μm and 174.3 ± 11.1 μm for Z-200 and Z-400, respectively (Fig. 5). Therefore, as expected, a thinner biofilm is observed on the Z-200 as compared to the Z-400. However, the measured biofilm thickness was approximately half of the maximum allowed biofilm thickness for the two Z-carriers. Even though the maximum biofilm thickness on Z-carriers is predefined by the grid wall height (200 μm for the Z-200 carrier and 400 μm for the Z-400 carrier), the biofilm growth can also be limited by substrate availability, shear force or carrier interaction dynamics in the reactor, as with any other carriers.

In this study, it was observed that the biofilm thicknesses often varied from one side of the Z-carrier to the other side of the same carrier (Fig. 6b and c). In particular, a thicker and more uniform biofilm was observed to be formed on one side of the Z-carriers with a thinner biofilm on the other side of the same carrier. The differences in biofilm thickness between two sides of a carrier were more recognizable on the Z-400 carriers as compared to the Z-200. This phenomenon may have been the result of different reasons such as the carriers mould, the tendency of Z-carriers in the reactor to stack in pairs and the scraping depth, which lead to a thinner biofilm in the center of each compartment.[40] Although the continuous aeration in the reactor keeps the carriers in constant movement, it was observed in this study

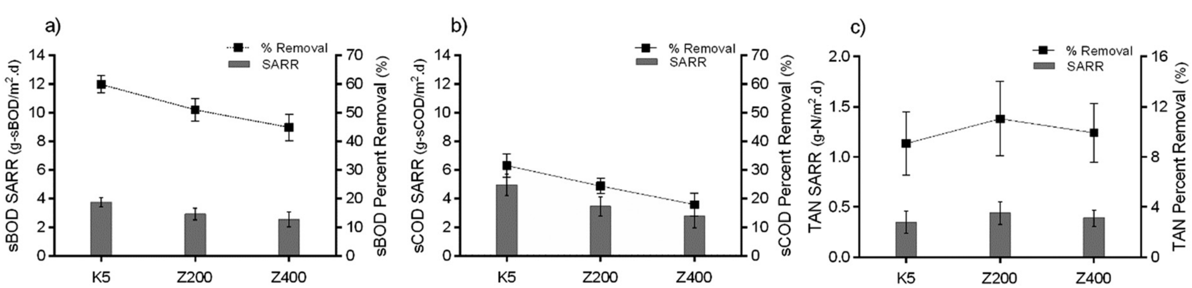

Fig. 4 SARR and percent removal at SALR of 6.0 ± 0.8 g-sBOD m^{-2} d^{-1} for (a) sBOD (b) sCOD and (c) TAN removal.

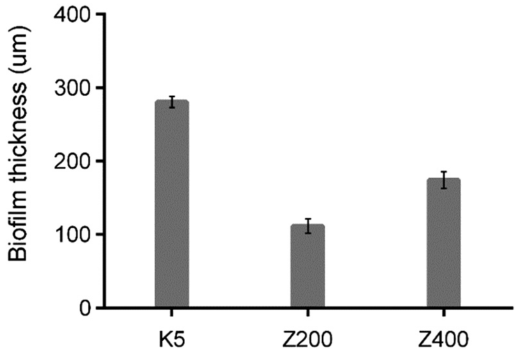

Fig. 5 Biofilm thickness of various carriers, average and 95% CI.

that likely due to the shape of the Z-carriers, some carriers may stack in pairs and move together as pairs in the reactor. Therefore, the depth of the biofilm being limited on one side of the carrier that may not have been exposed to an adequate substrate supply due to stacking. This effect may be due to the bench-scale size of the MBBR system used in this study and in particular an effect of the mixing dynamics of carriers in the small volume reactors. Similar to previous studies, thicker biofilm was observed along the grid walls and thinner biofilm towards the center of each compartment that could be explained as a result of the carriers scraping each other.[40] Therefore, thinner biofilm in the center of each compartment, as well as thinner biofilm on one side of some carriers, has likely resulted in both Z-200 and Z-400 carriers demonstrating the overall average biofilm thickness lower than the predefined maximum thickness. It should be noted that previous studies that measured biofilm thicknesses while carriers were submersed in water show that the overall average nitrifying biofilm thickness on Z-400 carriers was approximately the height of the Z-400 grid walls.[40,42]

Previous studies demonstrated that biofilm thickness and structure affect the performance of the MBBR,[33] where thicker biofilm with higher biofilm porosity may lead to deeper oxygen penetration depth.[42] Therefore, higher carbonaceous removal rates for the K5 carriers with the thickest biofilm, observed in this study, could be explained by the higher substrate availability and an increased bacteria activation at deeper layers of biofilm because of more porosity. On the other hand, the saddle-shaped Z-carriers, which are three-dimensional carriers as compared to flat K5 carriers, could be hit by the rising aeration bubbles and change moving direction more than K5. Therefore, the increase of turbulence in the reactor results in an elevated shear on the biofilm as the biofilm surface is more exposed in Z-carriers than K5 carriers.[42] Thus, thinner biofilm observed on Z-carriers might be an indication of potentially higher shear stress, which results in a denser biofilm on Z-carriers as compared to K5. Therefore, the possibility of inadequate substrate supply into the biofilm due to the carrier stacking, as well as thinner and denser biofilm, could limit the kinetics of the Z-reactors as compared to K5 (the difference in removal kinetics for different carrier types is shown in Fig. 4).

Overall, the investigation of the biofilm thickness indicates that carrier type, shape and physical properties significantly affect the biofilm thickness, as the thickest biofilm was observed on protected and non-limited voids of K5 carriers. The newly designed thickness-restraint Z-carriers demonstrate different thicknesses compared to the conventional K5 carriers. Hence, Z-carriers successfully restrain the biofilm thickness and maintain the biofilm thickness within predefined maximum values.

Solids concentration, production, detachment

TSS, VSS, solids production and detachment rate were measured for the three reactors under the same experimental conditions of an SALR of 6.0 ± 0.8 g-sBOD m^{-2} d^{-1}, an HRT of 1.1 hours along with consistent DO, pH, and temperatures (Table 3). The MBBR effluent TSS concentration is a combination of biologically produced solids, detached biofilm from the carriers, and influent suspended solids. Since the particulate matter in the influent wastewater can be assumed to remain unchanged in high flow rate MBBR systems, with HRT values lower than 2 hours, the effect of hydrolysis was deemed negligible in this study.[19] The TSS production is calculated as the difference

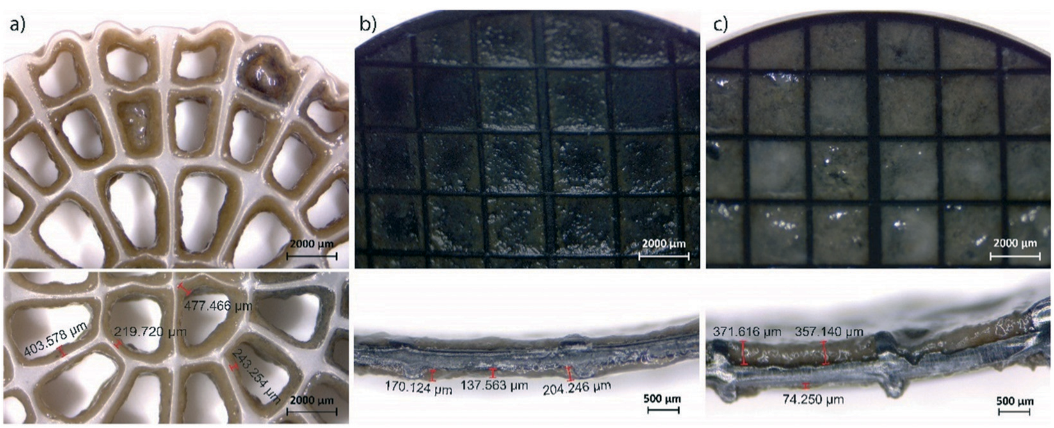

Fig. 6 Stereomicroscopy images of carriers showing biofilm thickness measurements, (a) top view of K5 carrier, (b) top view of Z-200 carrier and side view of cut Z-200 carrier, and (c) top view of Z-400 carrier and side view of cut Z-400 carrier.

between the effluent TSS and the influent TSS. The detachment rate is defined as the mass flux of the difference between the MBBR influent and effluent TSS and is normalized per reactor surface area. The lowest TSS, VSS, solids production and detachment rate were measured for K5 (Table 3). The K5 reactor solids production resulted in 7.7 ± 3.2 mg-TSS L^{-1} with a detachment rate of 1.7 ± 0.7 g-TSS m^{-2} d^{-1} solids, which is statistically significantly lower than the solids production and detachment rate of the Z-carrier systems. Therefore, it can be concluded that the carrier type has a significant impact on solids production and biofilm detachment rate.

On the other hand, the thickness-restraint carriers, comparison the Z-200 and Z-400 carriers, did not show a significant difference in the solids production and detachment rate. An average observed yield, defined as the production of TSS over the soluble substrate consumption, of 0.5 ± 0.2 g-TSS per g-$sBOD_{removed}$ was measured for K5, which is comparable with previous studies (0.12 to 0.56 g-TSS per g-$COD_{removed}$).[49] Moreover, 1.9 ± 0.7 and 1.6 ± 0.5 g-TSS per g-$sBOD_{removed}$ were measured for Z-200 and Z-400, respectively. Hence, the Z-carriers showed three times higher yields compared to K5 carriers. Since all three reactors were started at the same date and operated for 15 months, it is expected that the biofilm maturation on all carriers in this study was similar, and as such, differences in biofilm maturation did not affect the results. However, differences between the solids production and observed yield for different carrier type could be an important characteristic for downstream sludge treatment and subsequent biogas potential in full-scale applications.

Solids characteristics and settleability

The total suspended solids removal efficiency of a WRRF is highly dependent on the behaviour of the solids. The particle size distribution MBBR effluent solids along with MBBR effluent solids settled for 4 hours are presented in this section. DPA was performed directly on the effluent of the three reactors immediately after sampling and also after 4 hours of settling to mimic the secondary clarifier retention time at the full-scale WRRF where the reactors were operated. The study on the settleability of solids was conducted at an SALR of 6.0 ± 0.8 g-sBOD m^{-2} d^{-1} and a constant HRT of 1.1 hours. The particle size distribution curves in the range of 2–400 μm were graphed along with the corresponding bar graphs for particles larger than 400 μm, before (Fig. 7) and after settling (Fig. 8). The graphs show the average of triplicate measurements of total volume percentage of particles with 95% confidence intervals. The volume percentages for both unsettled and settled effluent solids were normalized by the total volume of the particles presented in the unsettled effluent to enable a comparison of the unsettled and settled solids.[10]

The integrated area under the particle distribution curves (Fig. 7a) shows that 38.4 ± 2.3%, 48.7 ± 1.4% and 47.3 ± 2% of the total volume of unsettled effluent particles in the K5, Z-200 and Z-400 reactors, respectively, existed in the range of 2–400 μm. Therefore, statistically significantly lower percent volume of particles between 2–400 μm (38.4 ± 2.3%) and accordingly significantly higher percent volume of particles larger than 400 μm (61.6 ± 2.3%) are observed for K5 as compared to Z-carriers. However, the thickness-restraint carriers do not show statistically significant differences between percent volume of particles for Z-200 and Z-400, neither for particles between 2–400 μm nor for particles larger than 400 μm (Fig. 7b). Generally, greater than 50% of the total solids volume was observed to be larger than 400 μm in all three reactors (Fig. 7b). However, previous studies have shown that approximately 20% of the total particles volume is larger than 400 μm for carbon removal systems using synthetic wastewater at various loading rates.[10] The interference of influent solids with produced solids in systems fed with real wastewaters, such as in this study, may result in the agglomeration of solids and hence a higher percentage of large particles.

The trend of all three particle size distribution curves is similar for unsettled effluent particles in the range of 150–400 μm. However, Z-carriers were shown to produce a larger quantity of particles smaller than 150 μm as compared to K5 (Fig. 7a). An obvious distinction between Z-carriers and K5 carriers was observed for unsettled effluent particle size distribution in the range of 2–150 μm, where there is less distinction when comparing the effects of thickness-restraint on the Z-carriers in this range (Fig. 7a).

In addition, the peak quantity of unsettled effluent particles in the range of 2–400 μm is shown to shift slightly towards smaller particles (Fig. 7a), and in accordance, a slight decrease in mean particle diameter is also observed for Z-carriers as compared to K5 carrier. Therefore, the measured mean particle diameter was 289 ± 20 μm for K5, 267 ± 10 μm for Z-200 and 271 ± 17 μm for Z-400. The mean particle diameter is the diameter of the particle for which 50% of a sample's volume is smaller than and 50% of a sample's volume is larger than this value. The unsettled mean particle diameter did not show a statistically significant difference for different carrier types ($p > 0.05$). However, after 4 hours of settling, the K5 showed a statistically significantly smaller mean particle diameter (38 ± 14 μm) as compared to the two Z-carriers ($p < 0.05$), which implies the potential of better

Table 3 Effluent solids concentration, production and detachment rate in MBBR reactors (n = 10)

	SALR (g-sBOD m^{-2} d^{-1})	TSS (mg L^{-1})	VSS (mg L^{-1})	Production (mg-TSS L^{-1})	Detachment rate (g-TSS m^{-2} d^{-1})
K5	6.0 ± 0.8	53.4 ± 8.5	42.2 ± 4.0	7.7 ± 3.2	1.7 ± 0.7
Z-200	6.0 ± 0.8	70.4 ± 13.0	53.3 ± 6.5	19.4 ± 7.6	5.0 ± 2.0
Z-400	6.0 ± 0.8	65.5 ± 10.5	50.9 ± 6.6	15.1 ± 4.0	3.7 ± 1.0

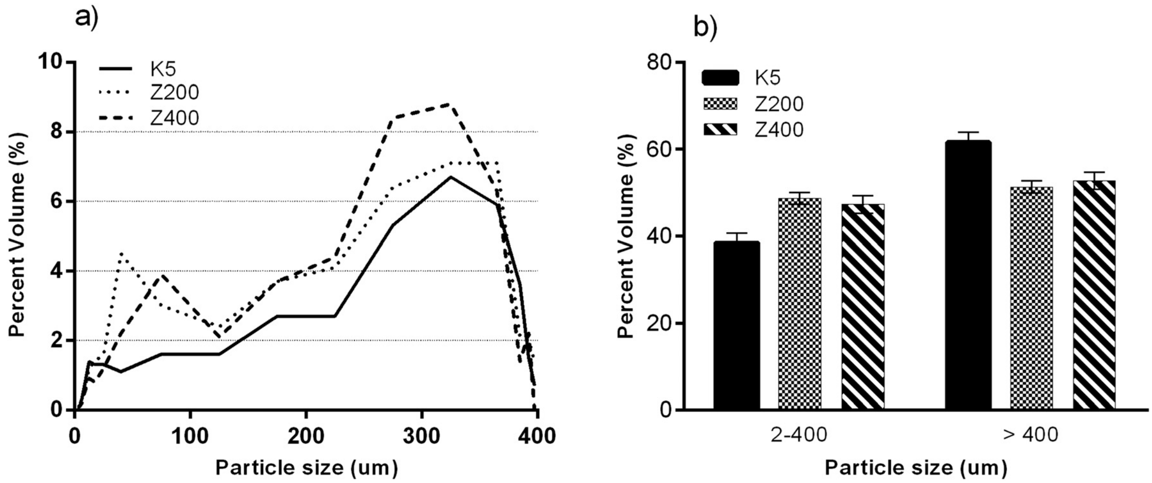

Fig. 7 Impact of different carriers on unsettled effluent particle distribution at SALR of 6 g-sBOD m^{-2} d^{-1}, (a) particle size distribution of particles between 2–400 μm, and (b) total volume percentages of particles smaller and larger than 400 μm.

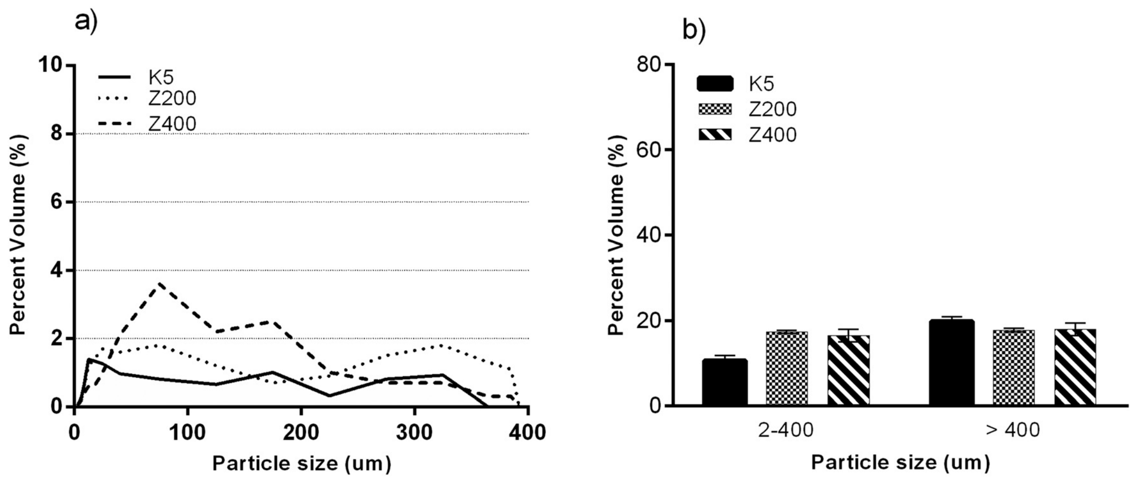

Fig. 8 Impact of different carriers on effluent particle distribution at SALR of 6 g-sBOD m^{-2} d^{-1} after 4 hours of settling, (a) particle size distribution of particles between 2–400 μm, and (b) total volume percentages of particles smaller and larger than 400 μm.

settling for solids detached from K5 carriers. The thickness-restraint carriers, comparison of Z-200 and Z-400, did not show a significant difference in the mean particle diameter after 4 hours of settling (96 ± 4 μm and 82 ± 11 μm for Z-200 and Z-400, respectively).

The settled particle distribution curves (Fig. 8) indicate that K5 contains a statistically significantly lower percent volume of particles between 2–400 μm (10.5 ± 1.2%) and larger than 400 μm (19.7 ± 1.1%) as compared to the Z-carriers. The lowest removal for all carriers occurred in the ranges of 2–200 μm particles, which implies the poor settleability of smaller particles (Fig. 8a). Furthermore, a large volume fraction of the particles is related to relatively large particles or aggregates of particles (in the range of 20–400 μm). Although the very small particles may not be the dominant volume fraction of particles, they may cause various challenges in solids separation.[20] The effect of carrier type on settleability indicates that the K5 carrier, with 69.7 ± 2.0% of total solids settling, showed statistically significantly higher settling efficiency compared to the Z-carriers. This can be explained by the larger particle size volume percentage of the particles and the distinct particle size distribution observed for the K5 carrier solids. As such, carrier design is herein shown to affect not only the quantity of particles detached from the carriers but also the size and settleability of the particles. On the other hand, the thickness-restraint effects of the Z-200 carrier compared to the Z-400 carriers did not significantly affect the settleability of the solids. Lower solids production, lower detachment rate (Table 3) and lower volume percentage of small particles indicate potentially better settleability for the K5 carrier. Although the small particles (2–150 μm) produced by Z-200 carriers appear to agglomerate and preferentially settle better than the small particles produced by Z-400 carriers, thickness-restraint Z-carriers did not differ significantly in terms of the overall settleability, as 65.0 ± 0.7% and 65.7 ± 1.1% of total solids settling was observed for Z-200 and Z-400, respectively. This demonstrates that carrier design, as opposed to thickness-restraint versions of similarly designed carriers, effects particle detachment and, in turn, the settleability of the effluent solids.

Conclusions

This study investigated the effects of carrier type and the biofilm thickness-restraint carrier design on the carbonaceous and TAN removal performance, biofilm thickness and subsequent solids production, particle characteristics and settleability. The application of various carriers at an SALR of 6.0 ± 0.8 g-sBOD m^{-2} d^{-1} and a constant HRT of 1.1 hours demonstrated that the carrier type has a significant effect on the carbonaceous removal rate (both sBOD and sCOD) and not a significant effect on TAN removal. TAN removal *via* nitrification was likely suppressed in all reactors due to the elevated carbonaceous loading of the reactors. Biofilm thickness-restraint was shown to not significantly affect the carbonaceous removal efficiency. The K5 carriers show lower TSS concentrations, lower solids production and lower detachment rates compared to the Z-carriers. The thickness-restraint carrier design of the Z-200 carrier and the corresponding thinner attached biofilm of the Z-200 carrier did not demonstrate statistically significant differences in solids production or biofilm detachment rate compared to the less thickness-restraint Z-400 carrier. The volume-based particle size distribution analysis of the MBBR effluent demonstrates a higher volume percentage of particles smaller than 400 μm for Z-carriers compared to K5 carriers. In particular, a significant distinction is observed in the particle size distribution range of 2–150 μm between the Z-carriers and the K5 carriers, which is likely related to the lower overall settleability of the Z-carriers effluent solids. As such, the carrier's physical properties have a significant effect on the solids production, detachment and subsequently the solids distribution size and settleability. In contrast, biofilm thickness and the restraint of biofilm thickness due to carrier design does not significantly affect the solids production, the detachment rate or the settling behaviour of the effluent solids.

Conflicts of interest

There are no conflicts to declare.

Acknowledgements

The authors would like to acknowledge the city of Gatineau, Quebec, Canada and Veolia Water Technologies Canada for their contribution to the research. Peter Vanrolleghem holds the Canada Research Chair in Water Quality Modelling.

References

1 D. Di Trapani, G. Mannina, M. Torregrossa and G. Viviani, Quantification of kinetic parameters for heterotrophic bacteria via respirometry in a hybrid reactor, *Water Sci. Technol.*, 2010, **61**, 1757–1766.
2 R. A. Dias, R. C. Martins, L. M. Castro and R. M. Quinta-Ferreira, in *WASTES - Solutions, Treatments and Opportunities II*, CRC Press, 2017, pp. 271–276.
3 C. Gazette, *Wastewater systems effluent regulations, Part II*, 2012, vol. 145, pp. 1632–1812.
4 M. Mannacharaju, P. Natarajan, A. K. Villalan, M. Jothieswari, S. Somasundaram and S. Ganesan, An innovative approach to minimize excess sludge production in sewage treatment using integrated bioreactors, *J. Environ. Sci.*, 2018, **67**, 67–77.
5 B. Young, R. Delatolla, T. Abujamel, K. Kennedy, E. Laflamme and A. Stintzi, Rapid start-up of nitrifying MBBRs at low temperatures: nitrification, biofilm response and microbiome analysis, *Bioprocess Biosyst. Eng.*, 2017, **40**, 731–739.
6 R. A. Delatolla and S. Babarutsi, Parameters affecting hydraulic behavior of aerated lagoons, *J. Environ. Eng.*, 2005, **131**, 1404–1413.
7 R. Delatolla, N. Tufenkji, Y. Comeau, A. Gadbois, D. Lamarre and D. Berk, Investigation of laboratory-scale and pilot-scale attached growth ammonia removal kinetics at cold temperature and low influent carbon, *Water Qual. Res. J. Can.*, 2010, **45**, 427–436.
8 B. Young, R. Delatolla, B. Ren, K. Kennedy, E. Laflamme and A. Stintzi, Pilot-scale tertiary MBBR nitrification at 1°C: characterization of ammonia removal rate, solids settleability and biofilm characteristics, *Environ. Technol.*, 2016, **37**, 2124–2132.
9 H. Ødegaard, A road-map for energy-neutral wastewater treatment plants of the future based on compact technologies (including MBBR), *Front. Environ. Sci. Eng.*, 2016, **10**, 2.
10 M. S. Karizmeh, R. Delatolla and R. M. Narbaitz, Investigation of settleability of biologically produced solids and biofilm morphology in moving bed bioreactors (MBBRs), *Bioprocess Biosyst. Eng.*, 2014, **37**, 1839–1848.
11 H. Ødegaard, B. Rusten and T. Westrum, A new moving bed biofilm reactor: applications and results, *Water Sci. Technol.*, 1994, **29**, 157–165.
12 J. P. Bassin and M. Dezotti, in *Advanced Biological Processes for Wastewater Treatment*, Springer, 2018, pp. 37–75.
13 X. Tian and R. Delatolla, Meso and micro-scale effects of loading and air scouring on nitrifying bio-cord biofilm, *Environ. Sci.: Water Res. Technol.*, 2019, **5**, 1183–1190.
14 E. Loupasaki and E. Diamadopoulos, Attached growth systems for wastewater treatment in small and rural communities: A review, *J. Chem. Technol. Biotechnol.*, 2013, **88**, 190–204.
15 H. Ødegaard, Sludge minimization technologies - An overview, *Water Sci. Technol.*, 2004, **49**, 31–40.
16 N. A. Ramli and M. F. Abdul Hamid, in *2017 IEEE Conference on Energy Conversion*, 2017, pp. 207–211.
17 R. M. Ahl, T. Leiknes and H. Ødegaard, Tracking particle size distributions in a moving bed biofilm membrane

reactor for treatment of municipal wastewater, *Water Sci. Technol.*, 2006, **53**, 33–42.

18 WEF, *Moving Bed Biofilm Reactors: WEF Manual of Practice No. 35*, McGraw-Hill, New York, 2011.

19 I. Ivanovic and T. O. Leiknes, Particle separation in moving bed biofilm reactor: Applications and opportunities, *Sep. Sci. Technol.*, 2012, **47**, 647–653.

20 H. Ødegaard, M. Cimbritz, M. Christensson and C. P. Dahl, Separation of biomass from moving bed biofilm reactors (MBBRs), *Proceedings of the Water Environment Federation*, 2010, pp. 212–233.

21 H. Ødegaard, B. Gisvold and J. Strickland, The influence of carrier size and shape in the moving bed biofilm process, *Water Sci. Technol.*, 2000, **41**, 383–391.

22 F. Morgan-Sagastume, Biofilm development, activity and the modification of carrier material surface properties in moving-bed biofilm reactors (MBBRs) for wastewater treatment, *Crit. Rev. Environ. Sci. Technol.*, 2018, **48**, 439–470.

23 M. Chaali, M. Naghdi, S. K. Brar and A. Avalos-Ramirez, A review on the advances in nitrifying biofilm reactors and their removal rates in wastewater treatment, *J. Chem. Technol. Biotechnol.*, 2018, **93**, 3113–3124.

24 H. Ødegaard, Innovations in wastewater treatment: The moving bed biofilm process, *Water Sci. Technol.*, 2006, **53**, 17–33.

25 K. Shahot, A. Idris, R. Omar and H. M. Yusoff, Review on biofilm processes for wastewater treatment, *Life Sci. J.*, 2014, **11**, 11.

26 J. P. McQuarrie and J. P. Boltz, Moving bed biofilm reactor technology: process applications, design, and performance, *Water Environ. Res.*, 2011, **83**, 560–575.

27 F. A. Almomani and M. A. M. Khraisheh, Treatment of septic tank effluent using moving-bed biological reactor: Kinetic and biofilm morphology, *Int. J. Environ. Sci. Technol.*, 2016, **13**, 1917–1932.

28 J. Dias, M. Bellingham, J. Hassan, M. Barrett, T. Stephenson and A. Soares, Impact of carrier media on oxygen transfer and wastewater hydrodynamics on a moving attached growth system, *Chem. Eng. J.*, 2018, **351**, 399–408.

29 R. Delatolla, C. Seguin, S. Springthorpe, E. Gorman, A. Campbell and I. Douglas, Disinfection byproduct formation during biofiltration cycle: Implications for drinking water production, *Chemosphere*, 2015, **136**, 190–197.

30 A. Barwal and R. Chaudhary, To study the performance of biocarriers in moving bed biofilm reactor (MBBR) technology and kinetics of biofilm for retrofitting the existing aerobic treatment systems: A review, *Rev. Environ. Sci. Bio/Technol.*, 2014, **13**, 285–299.

31 B. Patry, É. Boutet, S. Baillargeon and P. Lessard, Solid-liquid separation of an effluent produced by a fixed media biofilm reactor, *Water Sci. Technol.*, 2018, **77**, 589–596.

32 J. P. Bassin, I. N. Dias, S. M. S. Cao, E. Senra, Y. Laranjeira and M. Dezotti, Effect of increasing organic loading rates on the performance of moving-bed biofilm reactors filled with different support media: Assessing the activity of suspended and attached biomass fractions, *Process Saf. Environ. Prot.*, 2016, **100**, 131–141.

33 D. Forrest, R. Delatolla and K. Kennedy, Carrier effects on tertiary nitrifying moving bed biofilm reactor: An examination of performance, biofilm and biologically produced solids, *Environ. Technol.*, 2016, **37**, 662–671.

34 M. Levstek and I. Plazl, Influence of carrier type on nitrification in the moving-bed biofilm process, *Water Sci. Technol.*, 2009, **59**, 875–882.

35 B. Young, B. Banihashemi, D. Forrest, K. Kennedy, A. Stintzi and R. Delatolla, Meso and micro-scale response of post carbon removal nitrifying MBBR biofilm across carrier type and loading, *Water Res.*, 2016, **91**, 235–243.

36 E. Melin, T. Leiknes, H. Helness, V. Rasmussen and H. Ødegaard, Effect of organic loading rate on a wastewater treatment process combining moving bed biofilm and membrane reactors, *Water Sci. Technol.*, 2005, **51**, 421–430.

37 L. Chu and J. Wang, Comparison of polyurethane foam and biodegradable polymer as carriers in moving bed biofilm reactor for treating wastewater with a low C/N ratio, *Chemosphere*, 2011, **83**, 63–68.

38 R. K. Sonwani, G. Swain, B. S. Giri, R. S. Singh and B. N. Rai, A novel comparative study of modified carriers in moving bed biofilm reactor for the treatment of wastewater: Process optimization and kinetic study, *Bioresour. Technol.*, 2019, **281**, 335–342.

39 E. Ashrafi, E. Allahyari, E. Torresi and H. R. Andersen, Effect of slow biodegradable substrate addition on biofilm structure and reactor performance in two MBBRs filled with different support media, *Environ. Technol.*, 2019, DOI: 10.1080/09593330.2019.1581261.

40 M. Piculell, P. Welander, K. Jönsson and T. Welander, Evaluating the effect of biofilm thickness on nitrification in moving bed biofilm reactors, *Environ. Technol.*, 2016, **37**, 732–743.

41 M. Piculell, S. Lidén, G. Henningsson, F. Wessman, C. Thomson, T. Welander and M. Ekenberg, Minimizing Clogging and Scaling Issues in the Moving Bed Biofilm Reactor Using Biofilm Control, *Proc. Water Environ. Fed.*, 2016, **2015**, 4294–4303.

42 M. Piculell, *PhD thesis*, Lund University, 2016.

43 J. Schindelin, I. Arganda-Carreras, E. Frise, V. Kaynig, M. Longair, T. Pietzsch, S. Preibisch, C. Rueden, S. Saalfeld, B. Schmid and others, Fiji: an open-source platform for biological-image analysis, *Nat. Methods*, 2012, **9**, 676.

44 A. Siciliano and S. De Rosa, An experimental model of COD abatement in MBBR based on biofilm growth dynamic and on substrates' removal kinetics, *Environ. Technol.*, 2016, **37**, 2058–2071.

45 Y. Qiqi, H. Qiang and H. T. Ibrahim, Review on Moving Bed Biofilm Processes, *Pak. J. Nutr.*, 2012, **11**, 804–811.

46 L. Hem, B. Rusten and H. Ødegaard, Nitrification in a moving bed biofilm reactor, *Water Res.*, 1994, **28**, 1425–1433.

47 WEF, *Design of Municipal Wastewater Treatment Plants: WEF Manual of Practice No. 8*, McGraw-Hill, New York, 5th edn, 2009.

48 Metcalf & Eddy, *Wastewater Engineering: Treatment and Resource Recovery*, McGraw-Hill, New York, 5th edn, 2014.

49 C. Brosseau, B. Émile, M. A. Labelle, É. Laflamme, P. L. Dold and Y. Comeau, Compact secondary treatment train combining a lab-scale moving bed biofilm reactor and enhanced flotation processes, *Water Res.*, 2016, **106**, 571–582.